The cargo adaptor proteins RILPL2 and melanophilin co-regulate myosin-5a motor activity

Received for publication, January 2, 2019, and in revised form, June 3, 2019 Published, Papers in Press, June 7, 2019, DOI 10.1074/jbc.RA119.007384

Qing-Juan Cao[‡1], **Ning Zhang**[‡1], **Rui Zhou**[‡§], **Lin-Lin Yao**[‡], **and Xiang-dong Li**[‡§2]

From the [‡]*Group of Cell Motility and Muscle Contraction, State Key Laboratory of Integrated Management of Pest Insects and Rodents, Institute of Zoology, Chinese Academy of Sciences, Beijing 100101, China and the* [§]*University of Chinese Academy of Sciences, Beijing 100049, China*

Edited by Norma M. Allewell

Vertebrate myosin-5a is an ATP-utilizing processive motor associated with the actin network and responsible for the transport and localization of several vesicle cargoes. To transport cargo efficiently and prevent futile ATP hydrolysis, myosin-5a motor function must be tightly regulated. The globular tail domain (GTD) of myosin-5a not only functions as the inhibitory domain but also serves as the binding site for a number of cargo adaptor proteins, including melanophilin (Mlph) and Rab-interacting lysosomal protein–like 2 (RILPL2). In this study, using various biochemical approaches, including ATPase, single-molecule motility, GST pulldown assays, and analytical ultracentrifugation, we demonstrate that the binding of both Mlph and RILPL2 to the GTD of myosin-5a is required for the activation of myosin-5a motor function under physiological ionic conditions. We also found that this activation is regulated by the small GTPase Rab36, a binding partner of RILPL2. In summary, our results indicate that RILPL2 is required for Mlph-mediated activation of Myo5a motor activity under physiological conditions and that Rab36 promotes this activation. We propose that Rab36 stimulates RILPL2 to interact with the myosin-5a GTD; this interaction then induces exposure of the Mlph-binding site in the GTD, enabling Mlph to interact with the GTD and activate myosin-5a motor activity.

Vertebrate myosin-5a (Myo5a) is a processive motor that converts chemical ATP energy into mechanical power and moves continuously on the actin network (1). Myo5a can be structurally divided into four distinct regions: the N-terminal motor domain, six IQ motifs serving as the binding site for the light chains, the proximal tail comprising a series of coiled coils, and the C-terminal globular tail domain (GTD)[3] (2–5). The motor domain is the active domain containing the ATP-binding site and the actin-binding site. The tail portion, including the proximal tail and the GTD, serves as the binding site for the adaptor proteins. In addition, the GTD also functions as the inhibitory domain.

A tail inhibition model for the regulation of Myo5a motor function is widely accepted (2–5). In this model, Myo5a motor activity is activated by Ca^{2+} or cargo binding via adaptor proteins, and this activation is accompanied by a conformational transition of Myo5a from the folded conformation (~14 S) of the off state to the extended conformation (~11 S) of the on state (6–9). In the folded conformation, the GTD interacts with the motor domain and inhibits its motor function, whereas in the extended conformation, the motor domain is dissociated from the GTD and is fully active.

In vertebrate melanocytes, Myo5a is responsible for the transport and localization of the pigment organelle, the melanosome (10). Myo5a associates with melanosomes via melanophilin (Mlph) and the small GTPase Rab27a (11–15). Mlph interacts with both Rab27a and Myo5a, functioning as a linker between Rab27a and Myo5a (11, 13–15). Mlph contains two distinct Myo5a-binding regions, Mlph-GTBM (the GTD-binding motif of Mlph, residues 176–192) and Mlph-EFBD (the exon F–binding domain of Mlph, residues 241–400), which interact with the GTD and the melanocyte-specific alternative spliced exon F region in the proximal tail of Myo5a, respectively (9, 16–18).

The motor function of Myo5a can be activated by Mlph. Mlph stimulates the ATPase activity of Myo5a (18) and increases the number of processively moving Myo5a molecules (19). We demonstrated that Mlph-GTBM is sufficient for activation of the ATPase activity of Myo5a by disrupting the head–GTD interaction (9). However, all abovementioned activations of Myo5a by Mlph are observed only in the presence of elevated concentrations of salt (0.15–0.3 M KCl), suggesting that other unknown cellular factors might be required for the activation of Myo5a by Mlph (5). One candidate is RILPL2 (Rab-interacting lysosomal protein–like 2), a Rab-interacting lysosomal protein (RILP) family member. Mammalian cells express three RILP family proteins (RILP, RILPL1, and RILPL2), each of which contains two conserved regions, RH1 and RH2 (RILP homology region 1 and 2, respectively) (20). RILPL2 was first identified as a binding partner of Myo5a in the brain (21). Structural and biochemical studies show that the RH1 of RILPL2 can form a ternary complex with Myo5a-GTD and Mlph-GTBM (22), sug-

This work was supported by National Natural Science Foundation of China Grants 31672359, 31470791, and 31171367. The authors declare that they have no conflicts of interest with the contents of this article.

This article contains Movies S1–S4.

[1] Both authors contributed equally to this work.

[2] To whom correspondence should be addressed. Tel.: 86-10-6480-6015; E-mail: lixd@ioz.ac.cn.

[3] The abbreviations used are: GTD, globular tail domain; GTBM, GTD-binding motif of melanophilin; RILP, Rab-interacting lysosomal protein; cDNA, complementary DNA; GTPγS, guanosine 5′-3-*O*-(thio)triphosphate; PEP, phosphoenolpyruvate; CaM, calmodulin; WB, wash buffer; CBB, Coomassie brilliant blue.

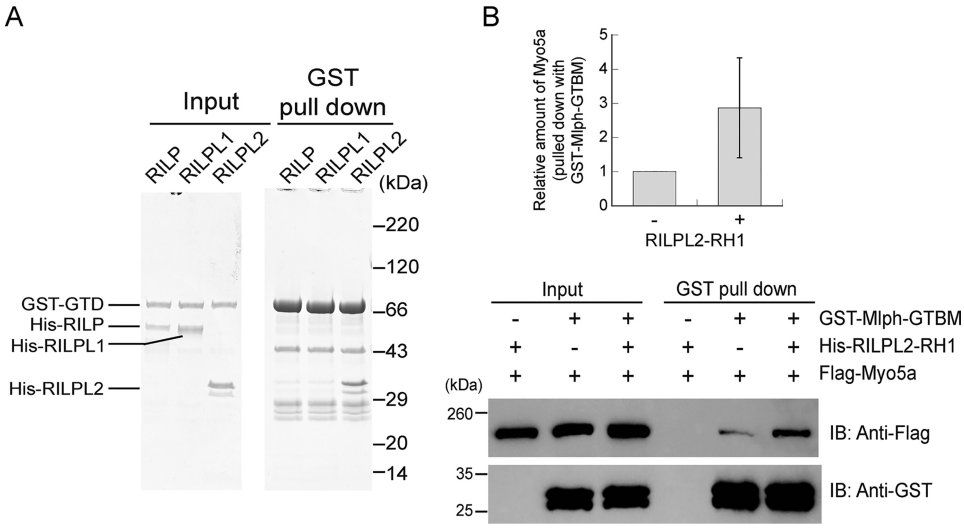

Figure 1. RILPL2 specifically interacts with Myo5a-GTD and enhances the interaction between Myo5a and Mlph-GTBM. *A*, Myo5a-GTD specifically interacts with RILPL2 but not RILP or RILPL1. Shown is GST pulldown of GST-Myo5a-GTD with RILP, RILPL1, and RILPL2. GST-Myo5a-GTD (2 μM) was incubated with 4 μM His-RILP, His-RILPL1, or His-RILPL2 and then pulled down by GSH-Sepharose. Inputs and pulldown samples were analyzed by SDS-PAGE (4%–20%) and visualized with CBB staining. The bands of ~43 kDa and ~26 kDa are the degradation of GST-GTD during the assay. *B*, RILPL2-RH1 enhances binding of Mlph-GTBM with Myo5a. FLAG-tagged full-length Myo5a (0.5 μM) was incubated with 2 μM GST-Mlph-GTBM and/or 2 μM His-RILPL2-RH1 and then pulled down using GSH-Sepharose. *Bottom panel*, the inputs and the pulldown samples were analyzed by Western blotting with the indicated antibodies. *Top panel*, the amount of Myo5a pulled down in the presence of RILPL1-RH1 relative to the absence of RILPL2-RH1 (data are the mean ± S.D. of three independent assays). *IB*, immunoblot.

gesting that RILPL2 might cooperate with Mlph in regulating the motor function of Myo5a.

In this work, we found that, similar to Mlph, RILPL2 is expressed in mouse melanocytes and demonstrated that both Mlph and RILPL2 are required for the activation of Myo5a motor function under physiological ionic strength. Moreover, the RILPL2/Mlph-GTBM activation of Myo5a motor function is stimulated by Rab36, a binding protein of RILPL2. These results indicate that RILPL2 and Rab36 play a key role in regulating Myo5a motor function.

Results

RILPL2-RH1 substantially increased the interaction between Myo5a and Mlph-GTBM

We first examined the expression of three RILP family proteins (RILP, RILPL1, and RILPL2) in melanocytes. The cDNAs of the three RILP family proteins were amplified by RT-PCR from mouse melanocytes, melan-a cells. DNA sequencing showed that these cDNAs are consistent with the reported sequences, indicating that all three RILP family proteins are expressed in melan-a cells. We then cloned the cDNAs of these three RILP family proteins into bacterial expression vectors. All three RILP family proteins, containing an N-terminal GST tag or His tag, were expressed in *Escherichia coli* and purified by GSH-Sepharose or Ni-agarose chromatography. To test the interactions between RILP family proteins with Myo5a, we performed a GST pulldown assay. As shown in Fig. 1*A*, RILPL2, but not RILP or RILPL1, was specifically pulled down with GST-tagged Myo5a-GTD. These results are consistent with the previous finding that Myo5a-GTD specifically interacts with RILPL2-RH1 but not with RILP-RH1 (22).

Because Myo5a-GTD, RILPL2-RH1, and Mlph-GTBM can form a ternary complex (22), we hypothesized that RILPL2-RH1 might enhance the interaction between Myo5a and Mlph-GTBM. To test this possibility, we produced His-tagged RILPL2-RH1 (residues 1–97), a truncated RILPL2 containing the conserved RH1. We then performed GST pulldown of GST-tagged Mlph-GTBM with FLAG-tagged Myo5a in the absence or presence of His-tagged RILPL2-RH1. The pulled down GST-Mlph-GTBM and FLAG-tagged full-length Myo5a were analyzed by SDS-PAGE and Western blotting. As shown in Fig. 1*B*, RILPL2-RH1 substantially increased the amount of FLAG-Myo5a pulled down with GST-tagged Mlph-GTBM.

Myo5a motor function is co-activated by RILPL2 and Mlph-GTBM

We hypothesized that RILPL2-RH1 and Mlph-GTBM might co-regulate the motor function of Myo5a. To test this possibility, we examined Mlph-GTBM activation of the actin-activated ATPase activity (hereafter referred to as ATPase activity) of Myo5a in the absence or presence RILPL2-RH1 under physiological ionic strength conditions, *i.e.* in the presence of 100 mM KCl. As shown in Fig. 2*A*, 5 μM RILPL2-RH1 had little effect on Myo5a ATPase activity but substantially increased the V_{max} and decreased the K_d of Myo5a ATPase activity activated by Mlph-GTBM. In the absence of RILPL2-RH1, Myo5a ATPase activity was activated by Mlph-GTBM with a V_{max} of 2.97 ± 0.35 s^{-1} $head^{-1}$ and a K_d of 30.1 ± 7.6 μM. In the presence of 5 μM RILPL2-RH1, Myo5a ATPase activity was strongly activated by Mlph-GTBM, with a V_{max} of 5.73 ± 0.40 s^{-1} $head^{-1}$ and a K_d of 2.83 ± 0.37 μM.

We then examined the ionic strength dependence of RILPL2-RH1/Mlph-GTBM activation of Myo5a ATPase activity. As shown in Fig. 2*B*, activation of Myo5a ATPase activity by 40 μM Mlph-GTBM and/or 5 μM RILPL2-RH1 is highly dependent on ionic strength. Myo5a ATPase activity in the absence of Mlph-GTBM and RILPL2-RH1 fluctuated in a narrow range over different KCl concentrations. In the presence of 5 μM

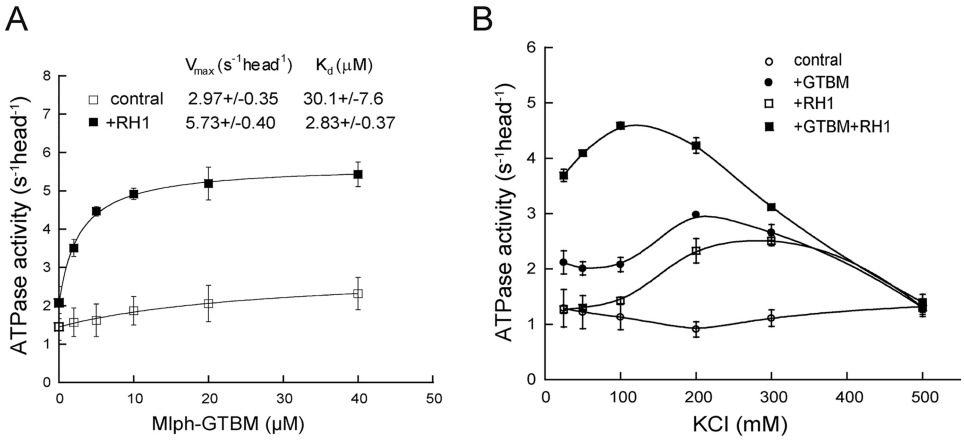

Figure 2. RILPL2-RH1 enhances the activation of Myo5a ATPase activity by Mlph-GTBM. *A*, activation of Myo5a ATPase activity by Mlph-GTBM in the absence or presence of RILPL2-RH1. The ATPase activity of Myo5a was measured in the presence of 0–40 μM Mlph-GTBM under EGTA conditions (20 mM MOPS-KOH (pH 7.0), 100 mM KCl, 1 mM DTT, 1 mM $MgCl_2$, 0.25 mg/ml BSA, 2.5 mM PEP, 20 units/ml pyruvate kinase, 12 μM CaM, 0.5 mM ATP, 40 μM actin, and 1 mM EGTA) in the absence (open *squares*) or presence (*closed squares*) of 5 μM RILPL2-RH1. V_{max} and K_d were obtained by a hyperbolic fit and are shown as means ± SDs from three independent assays. *B*, the effects of ionic strength on the activation of Myo5a ATPase activity by RILPL2-RH1 and Mlph-GTBM. The ATPase activity of Myo5a was determined under EGTA conditions and 25–500 mM KCl in the absence or presence of Mlph-GTBM and/or RILPL2-RH1. *Open circles*, in the absence of Mlph-GTBM and RILPL2; *closed circles*, in the presence of 40 μM Mlph-GTBM; *open squares*, in the presence of 5 μM His-RILPL2-RH1; *closed squares*, in the presence of 20 μM Mlph-GTBM and 5 μM His-RILPL2-RH1. All data are means ± SDs from three independent assays.

RILPL2-RH1 or 40 μM Mlph-GTBM, Myo5a ATPase activity was bell-shaped as a function of ionic strength, with a peak at 200–300 mM KCl. On the other hand, in the presence of both 5 μM RILPL2-RH1 and 40 μM Mlph-GTBM, Myo5a ATPase activity reached its climax around 100 mM KCl. These results indicate that both RILPL2-RH1 and Mlph-GTBM are required for activation of Myo5a motor function under physiological conditions.

To further analyze the activation of Myo5a by RILPL2-RH1 and Mlph-GTBM, we examined the motility activity of Myo5a at the single-molecule level. Cy3B-labeled Myo5a was first mixed with or without 20 μM Mlph-GTBM and/or 5 μM RILPL2-RH1 and then introduced into a flow chamber decorated with Alexa 488–labeled actin filaments. Images of Cy3B and Alexa 488 fluorescence were recorded under a total internal reflection fluorescence microscope (Fig. 3*A* and Movies S1–S4). In the absence of Mlph-GTBM and RILPL2-RH1, very few fluorescent spots of Cy3B-Myo5a colocalized and moved along actin filaments, and addition of Mlph-GTBM and RILPL2-RH1 caused a 13.1 ± 0.7–fold increase in the number of Myo5a molecules moving per time and length compared with Myo5a alone (Fig. 3*B*). On the other hand, addition of either Mlph-GTBM or RILPL2-RH1 alone did not greatly increase the number of Cy3B-Myo5a molecules moving along actin filaments. These results indicate that both Mlph-GTBM and RILPL2-RH1 are required for activation of Myo5a motor activity.

It is well established that activation of Myo5a ATPase activity by Ca^{2+} or adaptor proteins is accompanied by a conformational transition of Myo5a from the ~14 S folded conformation in the off state to the ~11 S extended conformation in the on state (6–9). We expected that RILPL2-RH1/Mlph-GTBM also induced the conformational transition of Myo5a. Therefore, we measured the S value of Myo5a in the presence of RILPL2-RH1 and/or Mlph-GTBM under physiological ionic strength (100 mM KCl) and in the absence of Ca^{2+} (in the presence of 1 mM EGTA). As shown in Fig. 4, the S value of Myo5a was 14.4 S and decreased to 12.2 S by 5 μM Mlph-GTBM and 5 μM RILPL2-RH1. On the other hand, 10 μM RILPL2-RH1 alone slightly increased the S value of Myo5a, and 10 μM Mlph-GTBM alone had little effect on it. These results indicate that, under physiological ionic strength and in the absence of Ca^{2+}, both Mlph-GTBM and RILPL2-RH1 are required for inducing Myo5a to form the extended conformation. Moreover, Myo5a might be more compact in the presence of RILPL2-RH1 than in its absence.

Rab36 stimulates RILPL2/Mlph-GTBM activation of Myo5a ATPase activity

RILPL2 contains two functional domains, RH1 and the RH2, which interact with Myo5a-GTD and Rab36, respectively (21, 23). To determine whether the interaction between RILPL2 and Rab36 depends on the nucleotide state of Rab36, we performed GST-RILPL2 pulldown with GTPγS-bound Rab36 (Rab36-GTPγS) or GDP-bound Rab36 (Rab36-GDP). As shown in Fig. 5*A*, more Rab36-GTPγS was pulled down with GST-RILPL2 than Rab36-GDP, indicating that the RILPL2–Rab36 interaction depends on the GTP-bound state of Rab36.

We then examined the effects of Rab36 on RILPL2/Mlph-GTBM–mediated activation of Myo5a. We found that Mlph-GTBM activation of Myo5a ATPase activity was strongly enhanced by 5 μM RILPL2-RH1 (Fig. 5*B*, *column 4*) but weakly by 5 μM RILPL2 (Fig. 5*B*, *column 6*), suggesting that RH2 inhibits RH1/Mlph-GTBM–mediated activation of Myo5a. Because Rab36-GTPγS binds to RH2, we suspected that Rab36-GTPγS might relieve RILPL2-RH2 inhibition of the interaction between RILPL2-RH1 and Myo5a-GTD, stimulating RILPL2/Mlph-GTBM activation of Myo5a ATPase activity. We therefore measured Myo5a ATPase activity in the presence of RILPL2, Mlph-GTBM, and Rab36-GTPγS. Consistent with our expectation, 20 μM Rab36-GTPγS significantly enhanced Myo5a ATPase activity in the presence of RILPL2 and Mlph-GTBM (Fig. 5*B*, *column 7*). As a control, 20 μM Rab36-GTPγS had little effect on Myo5a ATPase activity in the absence of Mlph-GTBM

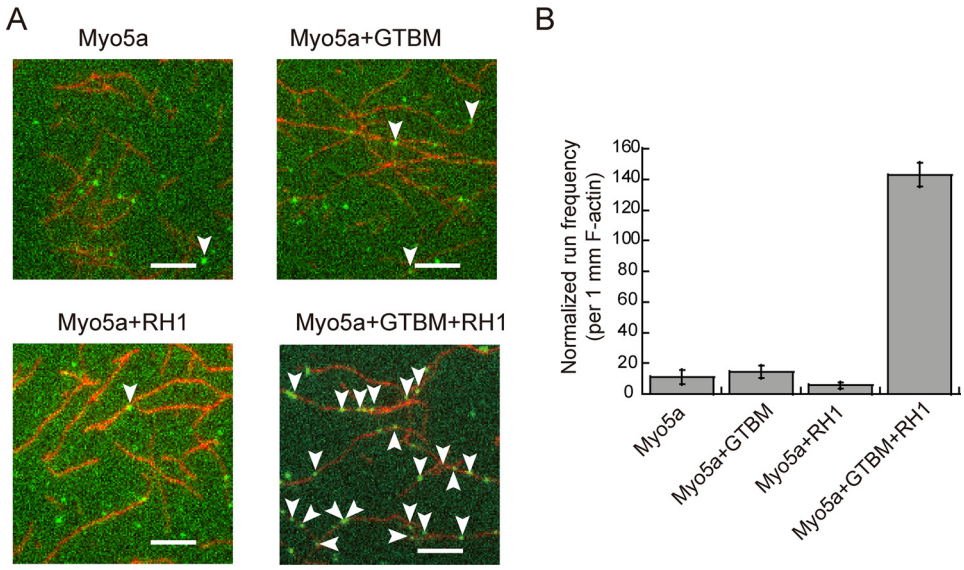

Figure 3. RILPL2-RH1 and Mlph-GTBM synergistically activate Myo5a motility activity. *A*, total internal reflection fluorescence microscopy images showing the movements of Myo5a molecules (*green*, Cy3B-Myo5a) along actin filaments (*red*, Alexa 488–labeled F-actin) in the absence or presence of 20 μM Mlph-GTBM and/or 5 μM RILPL2-RH1. The moving spots are indicated by *arrowheads* (see also Movies S1–S4). For clarity, only a part of the image (150 × 150 pixels) is shown. *Scale bars* = 5 μm. *B*, normalized frequency of Cy3B fluorescent spots moving along Alexa 488–labeled F-actin within a fixed time frame and area. Values are normalized to a 1-mm length of actin filament in 1 min. Values are means ± SDs of three different movies.

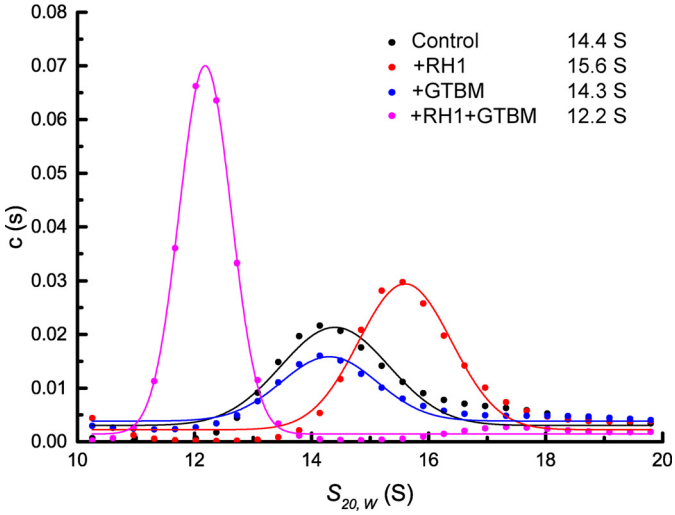

Figure 4. RILPL2-RH1 and Mlph-GTBM synergistically induce Myo5a to form the extended conformation. The S values of Myo5a (~2 μM Myo5a in 20 mM MOPS (pH 7.0), 100 mM KCl, 1 mM EGTA, 1 mM $MgCl_2$, and 1 mM DTT) in the absence or presence of RILPL2-RH1 and Mlph-GTBM were measured by analytical ultracentrifugation. *Control*, in the absence of RILPL2-RH1 and Mlph-GTBM; +*RH1*, in the presence of 10 μM RILPL2-RH1; +*GTBM*, in the presence of 10 μM Mlph-GTBM; +*RH1*+*GTBM*, in the presence of 5 μM RILPL2-RH1 and 5 μM Mlph-GTBM.

(Fig. 5*B*, *column 5*). These results indicate that Rab36 regulates RILPL2/Mlph-GTBM–mediated activation of Myo5a.

To further characterize the effects of Rab36 on the interaction between RILPL2 and Myo5a-GTD, we performed GST-Myo5a-GTD pulldown with RILPL2 and RILPL2-RH1 in the absence or presence of Rab36-GTPγS (Fig. 5*C*). We first compared the affinities of Myo5a-GTD with RILPL2 and RILPL2-RH1 using a GST pulldown assay. Both RILPL2 and the RILPL2-RH1 were stoichiometrically pulled down with GST-Myo5a-GTD (Fig. 5*C*, *lanes 7* and *8*), indicating strong interactions between Myo5a-GTD and RILPL2/RILPL2-RH1. However, a competition pulldown assay showed that RILPL2 has a lower affinity for Myo5a-GTD than RILPL2-RH1. When equal concentrations of RILPL2 and RILPL2-RH1 were present, significantly less RILPL2 was pulled down with GST-Myo5a-GTD than with RILPL2-RH1 (Fig. 5*C*, *lane 9*).

We then examined the effects of Rab36 on the interaction between RILPL2 and Myo5a-GTD using a competition pulldown assay. We found that 15 μM Rab36-GTPγS significantly increased the amount of RILPL2 pulled down but decreased that of RILPL2-RH1 (Fig. 5*C*, compare *lane 9* and *lane 10*). With Rab36-GTPγS increasing from 0 to 15 μM, the molar ratio of RILPL2 *versus* RILPL2-RH1 gradually increased from 0.28 ± 0.11 to 0.90 ± 0.18 (Fig. 5*C*, *right panel*). These results indicate that Rab36 regulates the interaction between RILPL2 and Myo5a-GTD.

Discussion

It is well established that the inhibited Myo5a is in a folded conformation, in which the GTD folds back to interact with the head, and the activated Myo5a is in an extended conformation, in which the head–GTD interaction is disrupted by Ca^{2+} or adaptor proteins (6–8, 24, 25). Mlph is one of the best-characterized adaptor proteins that are able to activate Myo5a (18, 19). However, under physiological ionic strength, Myo5a motor function was only weakly stimulated by Mlph or its truncation Mlph-GTBM (9, 18). This raises the possibility that other unidentified cellular factors might be required for the activation of Myo5a by Mlph (5). In this work, we demonstrated that RILPL2 is required for Mlph-mediated activation of Myo5a motor function under physiological ionic strength.

Structural and biochemical studies indicate that Myo5a-GTD forms a homodimer (Fig. 6*A*, *top*) in which the N-terminal extension of the GTD interacts with the Mlph-GTBM binding site in the counterpart GTD (26, 27). In other words, the Mlph-GTBM binding site is buried in the GTD–GTD interface. Thus, weakening the GTD–GTD interaction is expected to enhance

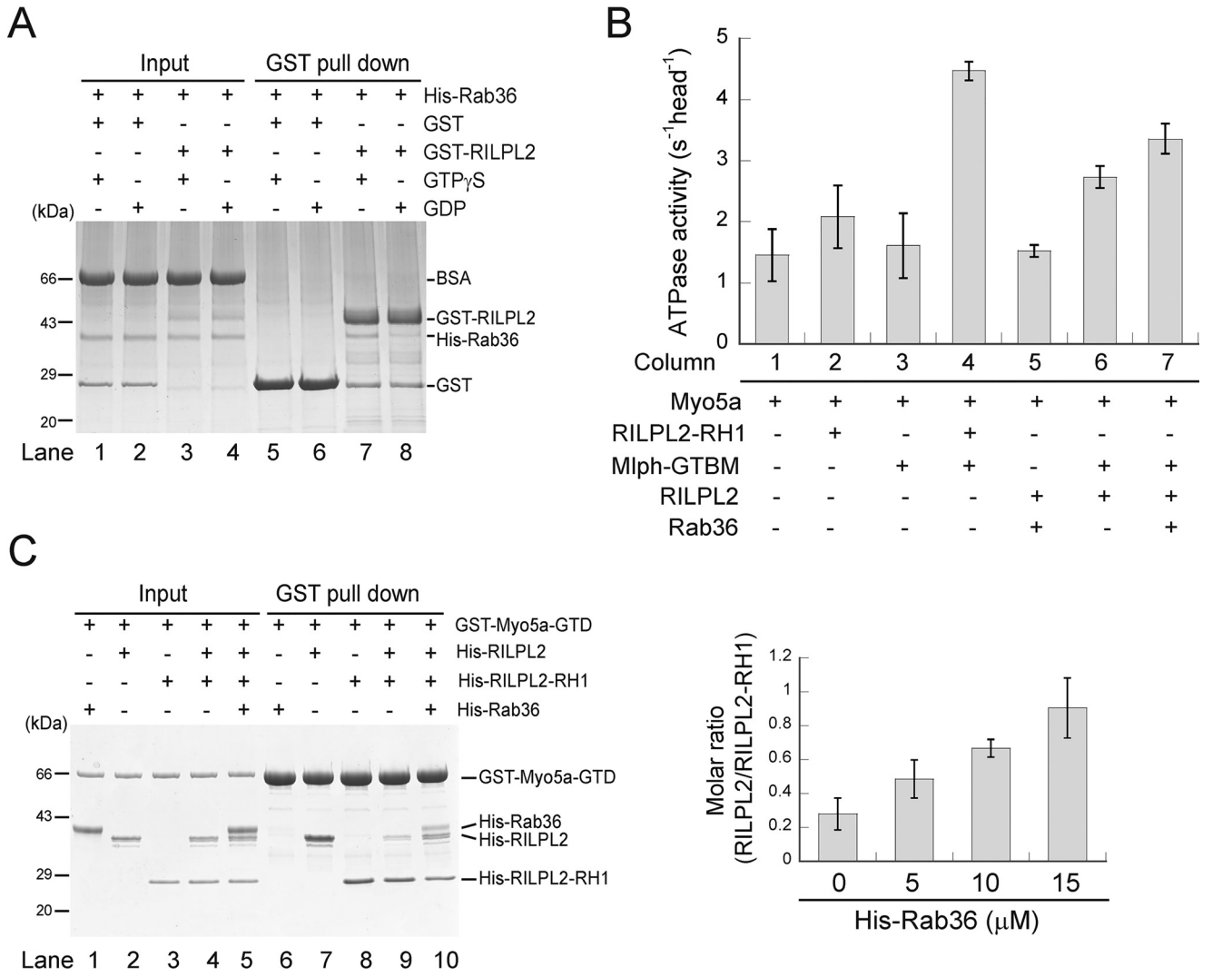

Figure 5. Rab36 stimulates Mlph-GTBM/RILPL2–mediated activation of Myo5a ATPase activity by enhancing RILPL2's interaction with Myo5a. *A*, Rab36 interacts with RILPL2 in a GTP-dependent manner. GST or GST-RILPL2 (20 μM, 20 μl) was bound onto 10 μl of GSH-Sepharose and then incubated with 200 μl of 2 μM His-Rab36 preloaded with GTPγS or GDP. The GSH-Sepharose–bound proteins were eluted by GSH and then analyzed by SDS-PAGE and visualized with CBB staining. *B*, the effects of Rab36 on Mlph-GTBM/RILPL2–mediated activation of Myo5a ATPase activity. The ATPase activity of Myo5a was measured under EGTA conditions as described in Fig. 1*A*, except that 5 μM His-RILPL2-RH1, 5 μM Mlph-GTBM, 5 μM His-RILPL2, and/or 20 μM Rab36-GTPγS were added. *C*, Rab36 enhances RILPL2's interaction with Myo5a-GTD. GST-Myo5a-GTD (4 μM) was incubated with 10 μM His-RILPL2 and/or 10 μM His-RILPL2-RH1 and/or 15 μM His-Rab36-GTPγS and then pulled down using GSH-Sepharose. *Left panel*, the inputs and the pulldown samples were separated by SDS-PAGE and visualized with CBB staining. *Right panel*, the molar ratio of RILPL2 *versus* RILPL2-RH1 pulled down with GST-Myo5a-GTD in the presence of 0–15 μM His-Rab36-GTPγS. The amounts of RILPL2 and RILPL2-RH-1 pulled down were quantified using the National Institutes of Health ImageJ program. The molar ratio of RILPL2 *versus* RILPL2-RH1 was calculated based on their molecular masses. Data are means ± SDs of at least three independent assays.

the activation of Myo5a by Mlph. Consistently, the activation of Myo5a by Mlph-GTBM is enhanced by the alanine mutations of the two conserved basic residues (Arg-1490 and Lys-1791), both of which participate in the GTD–GTD interaction (27). These findings lead us to propose that, in addition to the inhibited state and the activated state of Myo5a, there must be a third state, the preactivated state, which is similar to the inhibited state except that the Mlph-GTBM–binding site in the GTD dimer is exposed (27). We have proposed previously that the equilibrium of the inhibited state and the preactivated state of Myo5a is regulated by other unidentified cellular factors (5).

This work indicates that RILPL2 might be the unidentified cellular factor regulating the equilibrium between the inhibited state and the preactivated state of Myo5a. Crystal structures show that RILPL2-RH1, Myo5a-GTD, and Mlph-GTBM form a 2:2:2 hexamer comprising two Myo5a-GTD/Mlph-GTBM/RILPL2-RH1 trimers connected by the RILPL2-RH1 homodimer (Fig. 6*A*, *bottom*) (22). In contrast to the buried Mlph-GTBM–binding sites in the GTD–GTD dimer, the Mlph-GTBM–binding sites in the Myo5a-GTD/Mlph-GTBM/RILPL2-RH1 complex are located outside of the structure. Therefore, we expect that, upon binding with RILPL2-RH1, Myo5a-GTD will expose the Mlph-GTBM–binding site, facilitating the interaction with Mlph. Moreover, we found that Rab36 enhances the interaction between RILPL2 and Myo5a-GTD and stimulates the RILPL2/Mlph-GTBM–mediated activation of Myo5a, indicating that the RILPL2–Myo5a interaction is regulated by Rab36.

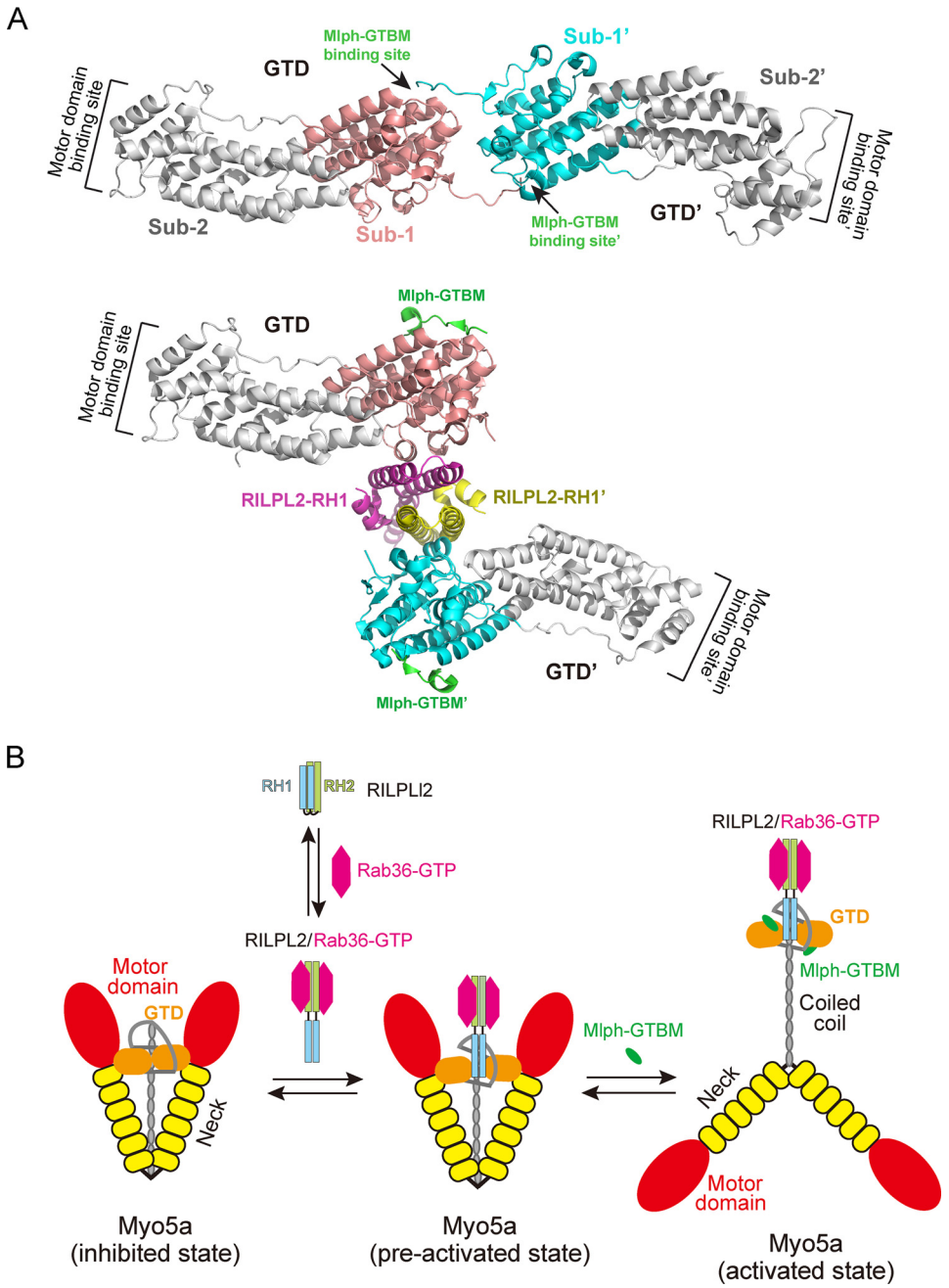

Figure 6. Proposed model for the regulation of Myo5a by RILPL2 and Mlph. *A*, the structures of the Myo5b-GTD homodimer and Myo5a-GTD/RILPL2-RH1/Mlph-GTBM ternary complex. *Top*, the structure of the Myo5b-GTD homodimer (PDB code 4J5M) formed by two symmetry-related molecules. *Bottom*, the structure of the Myo5a-GTD/RILPL2-RH1/Mlph-GTBM ternary complex (PDB code 4KP3). The Mlph-GTBM–binding site and the putative motor domain–binding site are indicated. *Sub-1* and *Sub-2* indicate subdomain 1 and 2 of Myo5a-GTD, respectively. *B*, a three-state model for the activation of Myo5a motor function by Rab36, RILPL2, and Mlph-GTBM. In the inhibited state, the two Myo5a-GTDs form a dimer and bind to the two heads of Myo5a, forming a triangular folded conformation. RILPL2 contains two domains, RH1 and RH2, which interact with Myo5a-GTD and the GTP-bound Rab36, respectively. In the absence of Rab36, RH2 prevents RH1 from binding to Myo5a-GTD. Binding of GTP-bound Rab36 to RH2 relieves RH2's inhibition on RH1. RH1 then binds to the GTD dimer of Myo5a in the inhibited state and induces the GTD to expose the Mlph-GTBM–binding site, forming the preactivated state. Finally, Mlph-GTBM binds to the Mlph-GTBM–binding site of Myo5a-GTD in the preactivated state and induces Myo5a to transform to the activated state in the extended conformation.

Based on the findings above and the three-state model of the regulation of Myo5a (27), we propose the following model for activation of Myo5a by Rab36, RILPL2, and Mlph (Fig. 6*B*). First, Rab36 binds to RILPL2-RH2, and this binding relieves the RILPL2-RH2 inhibition on RILPL2-RH1. RILPL2-RH1 then binds to Myo5a-GTD, exposing the Mlph-GTBM–binding site and transforming Myo5a from the inhibited state to the preactivated state. Finally, Mlph binds to Myo5a-GTD and allosterically inhibits the head–GTD interaction, transforming Myo5a from the preactivated state to the activated state.

A comparison of the crystal structures of the Myo5b-GTD dimer and the Myo5a-GTD/Mlph-GTBM/RILPL2-RH1 complex shows that the distance between the two putative motor domain–binding sites in the GTD dimer is decreased upon its binding to RILPL2-RH1 (Fig. 6*A*). This is consistent with the RILPL2-RH1–induced increase in Myo5a's S value (Fig. 4).

Therefore, we expect that Myo5a in the preactivated state is more compact than in the inhibited state.

The tail inhibition model for the regulation of myosin-5 by Ca^{2+} and adaptor proteins is well accepted, and many adaptor proteins of myosin-5 have been identified. However, so far, only two adaptor proteins of myosin-5, Mlph (9, 18, 19) and Rab11 (28, 29), have been shown to be able to activate myosin-5 motor function. Moreover, those activations are only observed under an elevated ionic strength. The current finding that both RILPL2 and Mlph are essential for activation of Myo5a motor function suggests that activation of class V myosin might require multiple adaptor proteins. Recently, it has been shown that Myo5a-GTD and two Myo5a adaptor proteins, Spir-2 and Rab11, might form a ternary complex (30). It is likely that Myo5a motor function is synergistically activated by Spir-2 and Rab11. Future experiments should clarify this issue.

Myo5a is essential for normal accumulation of melanosomes in dendritic tips in melanocytes, and its mutation causes perinuclear accumulation of melanosomes. Both Mlph and its interacting GTPase Rab27 are required for docking of Myo5a onto melanosomes and, lacking of either of them, a similar perinuclear accumulation of melanosomes (10–14, 31). Our finding suggests that RILPL2 and its interacting GTPase Rab36 cooperate with Mlph and Rab27 for docking of Myo5a onto melanosomes. It is possible that lack of either RILPL2 or Rab36 might also cause similar perinuclear accumulation of melanosomes in melanocytes.

RILP has been reported to mediate the association of dynein with late endosomes (32–33). Because both RILP and RILPL2 interact with Rab36 (23, 34), one possible scenario in melanocytes is that RILP-dynein and RILPL2-Myo5a compete with each other in associating with the melanosome-bound Rab36, regulating transport of melanosomes along microtubules and actin filaments. The roles of Rab36 and its effectors RILP and RILPL2 in the distribution and maturation of melanosomes in melanocytes deserve further investigation.

Experimental procedures

Materials

Restriction enzymes and Q5 high-fidelity DNA polymerase were purchased from New England Biolabs (Beverly, MA). Protease inhibitor mixture tablets were from Roche. The GoScript Reverse Transcription System Kit was from Promega. Ni-nitrilotriacetic acid–agarose (Ni-agarose) was from Qiagen. HRP-labeled anti-FLAG antibody, anti-FLAG M2 affinity agarose, phosphoenolpyruvate (PEP), 2,4-dinitrophenyl-hydrazine, and pyruvate kinase were from Sigma-Aldrich. GSH-Sepharose 4 Fast Flow (GSH-Sepharose) was from GE Healthcare. FLAG peptide (DYKDDDDK) was synthesized by Augct Co. (Beijing, China). Oligonucleotides were synthesized by Sunbiotech Co. Ltd. (Beijing, China). Actin was prepared from rabbit skeletal muscle acetone powder (35).

Proteins

The cDNAs of three RILP family proteins (RILP, RILPL1, and RILPL2) and Rab36 were cloned from melan-a cells by RT-PCR. Briefly, total RNAs were extracted from melan-a cells using TRIzol and reverse-transcribed to cDNA using the GoScript Reverse Transcription System Kit (Promega, A5000). The cDNAs of three RILP family proteins and Rab36 were amplified by PCR with melan-a cDNA as template and using the following primers: RILP, 5′-TAAGGATCCATGGAGCCCAGGAGGGCAGCGCCCAGGCTACCCAG-3′ (BamH1 site underlined) and 5′-ATTCTCGAGTCAGGAGTTGGGGGCTGGAGGGCTGTTCACAGGCTG-3′ (Xho1 site underlined); RILPL1, 5′-TAAGGTACCATGGAGGAGCCGCTAGGGTCACCGCC-3′ (Kpn1 site underlined) and 5′-ATTGGATCCTCACAGGTGCTGCAGGGCTTCCTGTCC-3′ (BamH1 site underlined); RILPL2, 5′-ACGCGGATCCATGGAGGATCACCCCGTG-3′ (BamHI site underlined) and 5′-ACCGCTCGAGCTAGGTATGCTTCCCTGAC-3′ (XhoI site underlined); Rab36, 5′-TTCGGATCCATGAGGTCCTCTTGGACCCCTTTG-3′ (BamH1 site underlined) and 5′-AATCTCGAGTTAACAGCAGCCTAGGCCGGGCGGCCTC-3′ (Xho1 site underlined). The resulting cDNAs were cloned into the pET30a vector (Novagen) or pGEX-4T2 vector (Amersham Biosciences). The cDNA of RILPL2-RH1 (RILPL2 residues 1–97) was amplified by PCR with RILPL2/pGEX-4T2 as a template using the primers 5′-ACGCGGATCCATGGAGGATCACCCCGTG-3′ (BamH1 site underlined) and 5′-TATCTCGAGTTAACCGGCTTTCCGCAGCCC-3′ (Xho1 site underlined) and subcloned into the pET30a vector. All clones were confirmed by DNA sequencing.

The recombinant proteins were expressed in BL21(DE3) *E. coli* as His-tagged proteins (in the pET30a vector) or GST-tagged proteins (in the pGEX-4T2 vector) and purified by Ni-agarose affinity chromatography or GSH-Sepharose affinity chromatography using standard procedures. FLAG-tagged Myo5a (full-length mouse melanocyte-type Myo5a) and GST-tagged Myo5a-GTD (comprising the C-terminal 410 residues of Myo5a) were prepared as described previously (36). Mlph-GTBM peptide (residues 176–201 of Mlph) and GST-tagged Mlph-GTBM were prepared as described previously (9). All protein concentrations in this study refer to the mole of polypeptide regardless of their oligomerization states.

ATPase assay

The ATPase activity of Myo5a was measured as described previously at 25 °C in an ATP regeneration system (36). The reaction buffer contained 20 mM MOPS-KOH (pH 7.0), 100 mM KCl, 1 mM $MgCl_2$, 1 mM DTT, 0.25 mg/ml BSA, 12 μM CaM, 0.5 mM ATP, 2.5 mM PEP, 20 units/ml pyruvate kinase, 1 mM EGTA, 40 μM actin, ~50 nM Myo5a, and indicated concentrations of other proteins, such as Mlph-GTBM, His-RILPL2, His-RILPL2-RH1, and His-Rab36.

Single-molecule motility assay

The single-molecule motility assay was performed at room temperature (~20 °C) in a 10-μl flow chamber in the absence of calcium as follows. Flow cells were incubated with 0.2 mg/ml *N*-ethylmaleimide–myosin in high-salt buffer (10 mM Hepes-KOH (pH 7.5), 500 mM KCl, and 5 mM $MgCl_2$) for 5 min, blocked with high-salt buffer plus 1 mg/ml casein for 5 min, and incubated with 0.04 μM Alexa 488–phalloidin–labeled actin filaments in low-salt buffer (20 mM Hepes-KOH (pH 7.6), 25 mM KCl, 2 mM $MgCl_2$, and 1 mM EGTA) for 3 min. After being rinsed with low-salt buffer plus 1 mg/ml casein, the flow cham-

ber was infused with the assay solution (~1 nM Cy3B-Myo5a, 12 μM CaM, 2000 units/ml catalase, 40 units/ml glucose oxidase, 6 mg/ml glucose, 10 μM ATP, 3.3 mM PEP, and 67 units/ml pyruvate kinase with or without 20 μM Mlph-GTBM and/or 5 μM RILPL2-RH1 in low-salt buffer). Images (512 × 512 pixels) were recorded at a frame rate of 5 s^{-1} using an inverted Nikon Ti-E total internal reflection fluorescence microscope as described previously (37). Images were merged and analyzed using the Matlab and ImageJ programs. The Cy3B fluorescent spots that moved along Alexa 488–phalloidin–labeled actin filaments were counted and normalized to the total length of actin filaments.

N-ethylmaleimide–myosin and Alexa 488–phalloidin–labeled actin filaments were prepared as described previously (37). CaM-A73C, a human CaM mutant created by site-directed mutagenesis, was expressed in *E. coli* and purified as described previously (38). CaM-A73C was labeled by Cy3B maleimide (GE Healthcare) as described previously (37). Cy3B-Myo5a was prepared by exchanging endogenous CaM with a 1:6 mixture of Cy3B-labeled CaM-A73C and WT CaM as described previously (39).

GST pulldown assay

GST pulldown assays were performed as described previously (27). All pulldown assays were repeated at least three times, and typical images are presented. In the GST-Mlph-GTBM/Myo5a pulldown assay, GSH-Sepharose beads (10 μl) were mixed with 95 μl of 2 μM GST-Mlph-GTBM, 0.5 μM FLAG-Myo5a, and 0 or 2 μM His-RILPL2-RH1 in wash buffer I (WB-I; 5 mM Tris-HCl (pH 7.5), 100 mM NaCl, 1 mM DTT, and 1 mM EGTA) and rotated at 4 °C for 2 h. The GSH-Sepharose beads were washed three times with 200 μl of WB-I and then eluted by 10 mM GSH, 50 mM Tris-HCl (pH 8.0), 1 mM DTT, and 200 mM NaCl. The eluted proteins were analyzed by SDS-PAGE (4%–20%) and visualized by Coomassie Brilliant Blue (CBB) staining or Western blotting using the indicated antibodies.

GST-RILPL2 pulldown with Rab36-GTPγS or -GDP was performed as follows. Rab36 was preloaded with nucleotides by incubating 2 μM His-Rab36 with 20 μM GTPγS or GDP in 1× PBS (12 mM sodium phosphate (pH7.4), 137 mM NaCl, and 27 mM KCl) containing 1 mg/ml BSA, 1 mM DTT, and 5 mM EDTA at 37 °C for 30 min before adding 10 mM $MgCl_2$ to stop the reaction. GST or GST-RILPL2 (20 μM, 20 μl) was bound onto GSH-Sepharose beads (10 μl) and then incubated with 200 μl of 2 μM His-Rab36-GTPγS or His-Rab36-GDP at 4 °C for 1 h. The GSH-Sepharose beads were washed with 200 μl of 1× PBS containing 1 mM DTT and 5 mM $MgCl_2$ five times and then eluted by 10 mM GSH, 50 mM Tris-HCl (pH8.0), 1 mM DTT, and 0.2 M NaCl. The eluted proteins were analyzed by SDS-PAGE (4%–20%) and visualized with CBB staining.

GST-Myo5a-GTD pulldown with RILPL2, RILPL2-RH1, and Rab36 was performed as follows. Rab36 was preloaded with GTPγS as described above, except that higher concentrations of Rab36 and GTPγS were used. GSH-Sepharose beads (10 μl) were mixed with 95 μl of 2 μM GST-Myo5a-GTD, 0–10 μM His-RILPL2, 0–10 μM His-RILPL2-RH1, and 0–15 μM His-Rab36-GTPγS in wash buffer II (WB-II; 5 mM Tris-HCl (pH 7.5), 150 mM NaCl, 1 mM DTT, and 1 mM EGTA) and rotated at 4 °C for 2 h. The GSH-Sepharose beads were washed three times with 200 μl of WB-II and then eluted by 10 mM GSH, 50 mM Tris-HCl (pH 8.0), 1 mM DTT, and 200 mM NaCl. The eluted proteins were analyzed by SDS-PAGE (4–20%) and visualized by CBB staining.

Analytical ultracentrifugation

The conformation of Myo5a was monitored by sedimentation velocity as described previously (9) with minor modifications (see below). About 2 μM Myo5a was first dialyzed against 20 mM MOPS-KOH (pH 7.0), 100 mM KCl, 1 mM DTT, and 1 mM EGTA at 4 °C overnight. Prior to running, 1 mM $MgCl_2$, 5 μM His-RILPL2-RH1, and 5 μM Mlph-GTBM peptide were added to the Myo5a sample. In control samples, 5 μM His-RILPL2-RH1 and 5 μM Mlph-GTBM peptide were replaced with H_2O, 10 μM His-RILPL2-RH1, or 10 μM Mlph-GTBM peptide. The sedimentation velocity was run at 40,000 rpm (20 °C) for 2 h in a Beckman Optima XL-I analytical ultracentrifuge. The sedimentation data were fitted to a continuous size distribution model in SEDFIT with a confidence level (F-ratio) of 0.68, where the frictional ratio (f/f_0) was allowed to float. The solvent viscosity and density were computed using SEDNTERP (40). The $c(s_{20,w})$ distributions were plotted using OriginPro 9.1.

Author contributions—Q.-J. C. and X.-d. L. data curation; Q.-J. C., N. Z., and X.-d. L. formal analysis; Q.-J. C., N. Z., R. Z., L.-L. Y., and X.-d. L. investigation; Q.-J. C. and X.-d. L. writing-original draft; Q.-J. C., N. Z., and X.-d. L. writing-review and editing; N. Z. methodology; R. Z. validation; X.-d. L. conceptualization; X.-d. L. resources; X.-d. L. supervision; X.-d. L. funding acquisition; X.-d. L. project administration.

References

1. Mehta, A. D., Rock, R. S., Rief, M., Spudich, J. A., Mooseker, M. S., and Cheney, R. E. (1999) Myosin-V is a processive actin-based motor. *Nature* **400,** 590–593 CrossRef Medline
2. Ikebe, M. (2008) Regulation of the function of mammalian myosin and its conformational change. *Biochem. Biophys. Res. Commun.* **369,** 157–164 CrossRef Medline
3. Sellers, J. R., Thirumurugan, K., Sakamoto, T., Hammer, J. A., 3rd, Knight, P. J. (2008) Calcium and cargoes as regulators of myosin 5a activity. *Biochem. Biophys. Res. Commun.* **369,** 176–181 CrossRef Medline
4. Trybus, K. M. (2008) Myosin V from head to tail. *Cell Mol. Life Sci.* **65,** 1378–1389 CrossRef Medline
5. Zhang, N., Yao, L. L., and Li, X. D. (2018) Regulation of class V myosin. *Cell Mol. Life Sci.* **75,** 261–273 CrossRef Medline
6. Wang, F., Thirumurugan, K., Stafford, W. F., Hammer, J. A., 3rd, Knight, P. J., and Sellers, J. R. (2004) Regulated conformation of myosin V. *J. Biol. Chem.* **279,** 2333–2336 CrossRef Medline
7. Krementsov, D. N., Krementsova, E. B., and Trybus, K. M. (2004) Myosin V: regulation by calcium, calmodulin, and the tail domain. *J. Cell Biol.* **164,** 877–886 CrossRef Medline
8. Li, X. D., Mabuchi, K., Ikebe, R., and Ikebe, M. (2004) Ca^{2+}-induced activation of ATPase activity of myosin Va is accompanied with a large conformational change. *Biochem. Biophys. Res. Commun.* **315,** 538–545 CrossRef Medline
9. Yao, L. L., Cao, Q. J., Zhang, H. M., Zhang, J., Cao, Y., and Li, X. D. (2015) Melanophilin stimulates myosin-5a Motor function by allosterically inhibiting the interaction between the head and tail of myosin-5a. *Sci. Rep.* **5,** 10874 CrossRef Medline

10. Wu, X., Bowers, B., Rao, K., Wei, Q., and Hammer, J. A., 3rd (1998) Visualization of melanosome dynamics within wild-type and dilute melanocytes suggests a paradigm for myosin V function *in vivo*. *J. Cell Biol.* **143,** 1899–1918 CrossRef Medline
11. Wu, X. S., Rao, K., Zhang, H., Wang, F., Sellers, J. R., Matesic, L. E., Copeland, N. G., Jenkins, N. A., and Hammer, J. A., 3rd. (2002) Identification of an organelle receptor for myosin-Va. *Nat. Cell Biol.* **4,** 271–278 CrossRef Medline
12. Wu, X., Wang, F., Rao, K., Sellers, J. R., and Hammer, J. A., 3rd (2002) Rab27a is an essential component of melanosome receptor for myosin Va. *Mol. Biol. Cell* **13,** 1735–1749 CrossRef Medline
13. Fukuda, M., Kuroda, T. S., and Mikoshiba, K. (2002) Slac2-a/melanophilin, the missing link between Rab27 and myosin Va: implications of a tripartite protein complex for melanosome transport. *J. Biol. Chem.* **277,** 12432–12436 CrossRef Medline
14. Strom, M., Hume, A. N., Tarafder, A. K., Barkagianni, E., and Seabra, M. C. (2002) A family of Rab27-binding proteins: melanophilin links Rab27a and myosin Va function in melanosome transport. *J. Biol. Chem.* **277,** 25423–25430 CrossRef Medline
15. Nagashima, K., Torii, S., Yi, Z., Igarashi, M., Okamoto, K., Takeuchi, T., and Izumi, T. (2002) Melanophilin directly links Rab27a and myosin Va through its distinct coiled-coil regions. *FEBS Lett.* **517,** 233–238 CrossRef Medline
16. Fukuda, M., and Itoh, T. (2004) Slac2-a/melanophilin contains multiple PEST-like sequences that are highly sensitive to proteolysis. *J. Biol. Chem.* **279,** 22314–22321 CrossRef Medline
17. Geething, N. C., and Spudich, J. A. (2007) Identification of a minimal myosin Va binding site within an intrinsically unstructured domain of melanophilin. *J. Biol. Chem.* **282,** 21518–21528 CrossRef Medline
18. Li, X. D., Ikebe, R., and Ikebe, M. (2005) Activation of myosin Va function by melanophilin, a specific docking partner of myosin Va. *J. Biol. Chem.* **280,** 17815–17822 CrossRef Medline
19. Sckolnick, M., Krementsova, E. B., Warshaw, D. M., and Trybus, K. M. (2013) More than just a cargo adapter, melanophilin prolongs and slows processive runs of myosin Va. *J. Biol. Chem.* **288,** 29313–29322 CrossRef Medline
20. Wang, T., Wong, K. K., and Hong, W. (2004) A unique region of RILP distinguishes it from its related proteins in its regulation of lysosomal morphology and interaction with Rab7 and Rab34. *Mol. Biol. Cell* **15,** 815–826 CrossRef Medline
21. Lisé, M. F., Srivastava, D. P., Arstikaitis, P., Lett, R. L., Sheta, R., Viswanathan, V., Penzes, P., O'Connor, T. P., and El-Husseini, A. (2009) Myosin-Va-interacting protein, RILPL2, controls cell shape and neuronal morphogenesis via Rac signaling. *J. Cell Sci.* **122,** 3810–3821 CrossRef Medline
22. Wei, Z., Liu, X., Yu, C., and Zhang, M. (2013) Structural basis of cargo recognitions for class V myosins. *Proc. Natl. Acad. Sci. U.S.A.* **110,** 11314–11319 CrossRef Medline
23. Matsui, T., Ohbayashi, N., and Fukuda, M. (2012) The Rab interacting lysosomal protein (RILP) homology domain functions as a novel effector domain for small GTPase Rab36: Rab36 regulates retrograde melanosome transport in melanocytes. *J. Biol. Chem.* **287,** 28619–28631 CrossRef Medline
24. Li, X. D., Jung, H. S., Mabuchi, K., Craig, R., and Ikebe, M. (2006) The globular tail domain of myosin Va functions as an inhibitor of the myosin Va motor. *J. Biol. Chem.* **281,** 21789–21798 CrossRef Medline
25. Thirumurugan, K., Sakamoto, T., Hammer, J. A., 3rd, Sellers, J. R., and Knight, P. J. (2006) The cargo-binding domain regulates structure and activity of myosin 5. *Nature* **442,** 212–215 CrossRef Medline
26. Pylypenko, O., Attanda, W., Gauquelin, C., Lahmani, M., Coulibaly, D., Baron, B., Hoos, S., Titus, M. A., England, P., and Houdusse, A. M. (2013) Structural basis of myosin V Rab GTPase-dependent cargo recognition. *Proc. Natl. Acad. Sci. U.S.A.* **110,** 20443–20448 CrossRef Medline
27. Zhang, W. B., Yao, L. L., and Li, X. D. (2016) The globular tail domain of myosin-5a functions as a dimer in regulating the motor activity. *J. Biol. Chem.* **291,** 13571–13579 CrossRef Medline
28. Ji, H. H., Zhang, H. M., Shen, M., Yao, L. L., and Li, X. D. (2015) The motor function of *Drosophila melanogaster* myosin-5 is activated by calcium and cargo-binding protein dRab11. *Biochem. J.* **469,** 135–144 CrossRef Medline
29. Ji, H. H., Yao, L. L., Liu, C., and Li, X. D. (2018) Regulation of Myosin-5b by Rab11a and the Rab11 family interacting protein 2. *Biosci. Rep.* **39,** BSR20181252 CrossRef Medline
30. Pylypenko, O., Welz, T., Tittel, J., Kollmar, M., Chardon, F., Malherbe, G., Weiss, S., Michel, C. I., Samol-Wolf, A., Grasskamp, A. T., Hume, A., Goud, B., Baron, B., England, P., Titus, M. A., *et al.* (2016) Coordinated recruitment of Spir actin nucleators and myosin V motors to Rab11 vesicle membranes. *Elife* **5,** e17523 CrossRef Medline
31. Hume, A. N., Collinson, L. M., Rapak, A., Gomes, A. Q., Hopkins, C. R., and Seabra, M. C. (2001) Rab27a regulates the peripheral distribution of melanosomes in melanocytes. *J. Cell Biol.* **152,** 795–808 CrossRef Medline
32. Jordens, I., Fernandez-Borja, M., Marsman, M., Dusseljee, S., Janssen, L., Calafat, J., Janssen, H., Wubbolts, R., and Neefjes, J. (2001) The Rab7 effector protein RILP controls lysosomal transport by inducing the recruitment of dynein-dynactin motors. *Curr. Biol.* **11,** 1680–1685 CrossRef Medline
33. Johansson, M., Rocha, N., Zwart, W., Jordens, I., Janssen, L., Kuijl, C., Olkkonen, V. M., and Neefjes, J. (2007) Activation of endosomal dynein motors by stepwise assembly of Rab7-RILP-p150Glued, ORP1L, and the receptor βIII spectrin. *J. Cell Biol.* **176,** 459–471 CrossRef Medline
34. Chen, L., Hu, J., Yun, Y., and Wang, T. (2010) Rab36 regulates the spatial distribution of late endosomes and lysosomes through a similar mechanism to Rab34. *Mol. Membr. Biol.* **27,** 23–30 CrossRef Medline
35. Spudich, J. A., and Watt, S. (1971) The regulation of rabbit skeletal muscle contraction: I: biochemical studies of the interaction of the tropomyosin-troponin complex with actin and the proteolytic fragments of myosin. *J. Biol. Chem.* **246,** 4866–4871 Medline
36. Li, X. D., Jung, H. S., Wang, Q., Ikebe, R., Craig, R., and Ikebe, M. (2008) The globular tail domain puts on the brake to stop the ATPase cycle of myosin Va. *Proc. Natl. Acad. Sci. U.S.A.* **105,** 1140–1145 CrossRef Medline
37. Shen, M., Zhang, N., Zheng, S., Zhang, W. B., Zhang, H. M., Lu, Z., Su, Q. P., Sun, Y., Ye, K., and Li, X. D. (2016) Calmodulin in complex with the first IQ motif of myosin-5a functions as an intact calcium sensor. *Proc. Natl. Acad. Sci. U.S.A.* **113,** E5812–E5820 CrossRef Medline
38. Lu, Z., Ma, X. N., Zhang, H. M., Ji, H. H., Ding, H., Zhang, J., Luo, D., Sun, Y., and Li, X. D. (2014) Mouse myosin-19 is a plus-end-directed, high-duty ratio molecular motor. *J. Biol. Chem.* **289,** 18535–18548 CrossRef Medline
39. Trivedi, D. V., Muretta, J. M., Swenson, A. M., Davis, J. P., Thomas, D. D., and Yengo, C. M. (2015) Direct measurements of the coordination of lever arm swing and the catalytic cycle in myosin V. *Proc. Natl. Acad. Sci. U.S.A.* **112,** 14593–14598 CrossRef Medline
40. Lebowitz, J., Lewis, M. S., and Schuck, P. (2002) Modern analytical ultracentrifugation in protein science: a tutorial review. *Protein Sci.* **11,** 2067–2079 Medline